Two-nucleon system above pion threshold: Quark model study

D. R. Entem,[1,2] F. Fernández,[1] and A. Valcarce[1]
[1]*Nuclear Physics Group, University of Salamanca, E-37008 Salamanca, Spain*
[2]*Department of Physics, University of Idaho, Moscow, Idaho 83844*
(Received 27 September 2002; published 17 January 2003)

We present a study of the NN system above pion threshold fully based on a constituent quark model. The calculation is performed in the framework of the coupled-channel method. A $\pi N\Delta$ vertex has been derived from the basic πqq vertex and it is probed in the P_{33} πN partial wave. Taking into account the fact that this is a parameter-free calculation, the phase shifts and inelasticities are reasonably well reproduced.

DOI: 10.1103/PhysRevC.67.014001 PACS number(s): 12.39.Jh, 13.75.Cs, 14.20.Gk, 24.85.+p

I. INTRODUCTION

Constituent quark models have been used for a long time to investigate the nucleon-nucleon (NN) system. The first reliable explanation of the short-range part of the NN interaction was provided by the Fermi-Breit form of the one-gluon exchange [1]. Later on, the quark-quark (qq) interaction got supplemented by the exchange of Goldstone bosons when constituent quark masses were related to the spontaneous chiral symmetry breaking [2]. Within this approach, a reasonable description of the NN phase shifts below the pion threshold and the deuteron properties was obtained with a minimal set of parameters [3]. At the same time, the door to a coherent and simultaneous description of the baryon spectra was opened [4].

Above the pion threshold the Δ isobar is an important mode of nucleonic excitation. The interaction of the Δ isobar with nucleons is experimentally unobservable and theoretically unknown to a large extent. Thus the Δ isobar's effects on nuclear observables have to be studied theoretically and are model dependent. Quark-model-based interactions have been used to explore the two-nucleon system above the pion threshold in their dependence on a chosen nucleon-Δ potential [5]. In this study the basic nucleon-nucleon interaction was taken to be the Paris potential. However, a fully quark-model-based calculation of the two-nucleon system above the pion threshold has never been done.

Apart from the fundamental theoretical interest of describing the NN interaction in terms of basic degrees of freedom, there are also several specific reasons to undertake such a project. First of all, quark antisymmetrization gives a mechanism to generate short-range repulsion even for the less experimentally known systems ($N\Delta$, $\Delta\Delta$) in a completely parameter-free way. Second, quark degrees of freedom provide a unified way of treating consistently the nucleon and its resonances. These two aspects reduce the ambiguities with respect to the traditional meson-exchange approaches to study the NN system above the pion threshold.

Theoretically, the πNN system is usually studied by means of two different approaches [6]. The first one is the coupled πNN-NN approach (*PNNA*), where the necessary ingredients to solve the equations are the off-shell t matrices for the two-body πN and NN scattering. For technical reasons these two-body inputs are assumed to take separable forms. The second one is the coupled-channel method (CCM), which describes the physics above the pion threshold by means of two-body coupled-channel equations linking the NN state to NB and BB' channels, where $B(B')$ represents nucleon resonances. Once the decay width of the resonances is incorporated in the propagators, the equations are able to properly couple physical two (NN) and three (πNN) particle states. Though originating from distinct motivations, the final equations look quite similar. With a comparable set of input and kinematical assumptions the two approaches are almost identical except that in most CCM approaches the intermediate state with an interacting nucleon pair and a spectator pion is not included.

From a quark-model point of view, the nucleon is a composite system and the resonances correspond to its excited states. Therefore the coupled-channel method seems to be a natural framework to study the πNN system using quark degrees of freedom. Experimentally, it can be observed that the inelasticity in two-nucleon scattering up to at least 500 MeV in the c.m. system, i.e., far beyond the two-pion threshold, is predominantly single-pion production and occurs essentially in the isospin-triplet partial waves. These experimental facts suggest pion production in intermediate-energy two-nucleon scattering to proceed through single-Δ excitation. Processes like double-Δ excitation with subsequent production of two pions appear to be suppressed in the considered energy region. The experimentally suggested restriction to single-Δ excitation is an enormous technical simplification [7]. Only the interaction in the isospin-triplet two-nucleon partial waves gets modified by the additional Δ-isobar and pion degrees of freedom, the isospin-singlet partial waves are described usually by a purely nucleonic potential.

In this work we will make use of the quark model presented in Ref. [3] to study the NN system above the pion threshold using the coupled-channel method. The paper is organized as follows. In Sec. II we briefly review the constituent quark model. Section III is devoted to the construction of the $\pi N\Delta$ vertex that will be used in Sec. IV to calculate the P_{33} πN phase shift. The coupled-channel method at the quark level is developed in Sec. V. Section VI is dedicated to presenting and discussing the results. Finally, we summarize the most important conclusions in Sec. VII.

II. THE CONSTITUENT QUARK MODEL

The constituent quark model used in this work has been extensively described elsewhere [2,3] and therefore we will

only summarize here its most relevant aspects. The chiral symmetry of the original QCD Lagrangian appears spontaneously broken in nature and as a consequence light quarks acquire a dynamical mass. The simplest Lagrangian invariant under chiral rotations must therefore contain chiral fields, and can be expressed as

$$\mathcal{L}=\bar{\psi}[i\partial\!\!\!/-M(q^2)U^{\gamma_5}]\psi, \tag{1}$$

where $U^{\gamma_5}=e^{i(\lambda_a/f_\pi)\phi^a\gamma_5}$ is the Goldstone boson fields matrix and $M(q^2)$ the dynamical (constituent) mass. This Lagrangian has been derived in Ref. [8] as the low-energy limit in the instanton liquid model. In this model the dynamical mass vanishes at large momenta and it is frozen at low momenta, for a value around 300 MeV. Similar results have also been obtained in lattice calculations [9]. To simulate this behavior we parametrize the dynamical mass as $M(q^2)=m_q F(q^2)$, where $m_q\simeq$ 300 MeV, and

$$F(q^2)=\left[\frac{\Lambda_\chi^2}{\Lambda_\chi^2+q^2}\right]^{1/2}. \tag{2}$$

The cutoff Λ_χ fixes the chiral symmetry breaking scale. Following Manohar and Georgi [10] and taking into account that this scale is larger than the confinement scale, QCD reduces to an effective low-energy theory of confined constituent quarks interacting through elementary chiral fields.

If we restrict ourselves to SU(2), U^{γ_5} can be written as $U^{\gamma_5}=e^{i\gamma_5\vec{\tau}\cdot\vec{\phi}/f_\pi}$. We will assume that the Goldstone boson of the theory is the pion and therefore the expansion of U^{γ_5} provides a quark-quark interaction through virtual pion exchanges. Defining the auxiliary fields

$$\vec{\pi}=\vec{\phi}f_\pi\sin(\phi/f_\pi), \tag{3}$$

$$\sigma=f_\pi[\cos(\phi/f_\pi)-1]. \tag{4}$$

one arrives at the interaction Hamiltonian

$$\mathcal{H}_{ch}=g_{ch}F(q^2)\bar{\psi}(\sigma+i\gamma_5\vec{\pi}\cdot\vec{\tau})\psi, \tag{5}$$

where $g_{ch}=m_q/f_\pi$. From this Hamiltonian one can obtain the quark-quark interaction potentials due to the exchange of a scalar and a pseudoscalar Goldstone boson. The scalar boson exchange takes into account the most important part of the two-pion exchange. The potentials are given in momentum space by

$$V_{ij}^{PS}(\vec{q})=-\frac{1}{(2\pi)^3}\frac{g_{ch}^2}{4m_q^2}\frac{\Lambda_\chi^2}{\Lambda_\chi^2+q^2}\frac{(\vec{\sigma}_i\cdot\vec{q})(\vec{\sigma}_j\cdot\vec{q})}{m_{PS}^2+q^2}(\vec{\tau}_i\cdot\vec{\tau}_j), \tag{6}$$

$$V_{ij}^{S}(\vec{q})=-\frac{g_{ch}^2}{(2\pi)^3}\frac{\Lambda_\chi^2}{\Lambda_\chi^2+q^2}\frac{1}{m_S^2+q^2}, \tag{7}$$

where $\vec{q}$ is the momentum transfer, $\vec{\sigma}_i$ ($\vec{\tau}_i$) are the spin (isospin) Pauli matrices of quark i, m_q is the constituent quark mass, and m_{PS} (m_S) is the mass, of the pseudoscalar (scalar) boson.

Below the chiral symmetry breaking scale quarks still interact through gluon exchanges. How to match this interaction with the constituent quark picture is still not clarified. We shall assume that the gluon coupling freezes at some small value below the chiral symmetry breaking scale resulting in an effective interaction between constituent quarks described by the Lagrangian

$$\mathcal{L}_{gqq}=i\sqrt{4\pi}\alpha_s\bar{\psi}\gamma_\mu G_c^\mu\lambda_c\psi, \tag{8}$$

where λ_c are the SU(3) color generators and G_c^μ the gluon field. From this Lagrangian, de Rújula, Georgi, and Glashow [11] derived the one-gluon exchange in the nonrelativistic limit. It reads in momentum space as

$$V_{ij}^{OGE}(\vec{q})=\frac{1}{(2\pi)^3}\frac{1}{4}(\vec{\lambda}_i\cdot\vec{\lambda}_j)\;4\pi\alpha_s\times\left\{\frac{1}{q^2}-\frac{1}{4m_q^2}\left[1+\frac{2}{3}(\vec{\sigma}_i\cdot\vec{\sigma}_j)\right]+\frac{1}{4m_q^2}\frac{1}{q^2}[\vec{q}\otimes\vec{q}]^{(2)}\cdot[\vec{\sigma}_i\otimes\vec{\sigma}_j]^{(2)}\right\}, \tag{9}$$

where $\vec{\lambda}_i$ are the color Gell-Mann matrices of quark i and α_s is the strong coupling constant.

The other QCD nonperturbative effect corresponds to confinement, which prevents having colored hadrons. It is usually simulated by means of a phenomenological linear potential of the form $V_{ij}^{CON}=a(\vec{\lambda}_i\cdot\vec{\lambda}_j)r$. Confinement influences the spectrum, but its $\vec{\lambda}_i\cdot\vec{\lambda}_j$ structure avoids contributions to the baryon-baryon interaction.

Finally, we need an ansatz for the radial wave function of the quarks. It will be taken, as usual, as a ground-state harmonic oscillator wave function

$$\psi(\vec{r}_i)=\prod_{i=1}^{3}\left[\frac{1}{\pi b^2}\right]^{3/4}e^{-r_i^2/2b^2}. \tag{10}$$

III. FROM THE πqq TO $\pi BB'$ VERTEX

Within the constituent quark model, the decay of a baryon (B) into a meson-baryon state (M',B') is determined by the matrix element

$$\Gamma_{B'M',B}(\vec{k})=\langle\psi^{B'},\psi^{M'}|H_M(\vec{k})|\psi^B\rangle, \tag{11}$$

where $\psi^{B'(B)}$ is the baryon wave function and $H_M(\vec{k})$ is an appropriate operator describing how a meson M with momentum $\vec{k}$ is emitted by constituent quarks. A phenomenological model for $H_M(\vec{k})$ was developed in the 1970s by Le Yaouanc *et al.* [12] assuming that strong decays proceed by simple emission of a meson through one of the quarks of the

hadron, the so-called elementary emission model. The meson is not resolved into quarks and the pair creation that is, strictly speaking, necessary, for such a decay is concealed by the formalism. The main advantage of this model is simplicity. Moreover, relativistic kinematics can be maintained for the meson, while its resolution into quarks would naturally restrict us to the nonrelativistic approximation. This model has been widely applied to strong baryon decays.

As we have seen, our model includes a πqq vertex which arises as a QCD nonperturbative effect. Then we consider that $H_M(\vec{k})$ is a one-body operator which can be derived directly from the effective Lagrangian of Eq. (1). Following Le Yaouanc *et al.*, we perform a nonrelativistic reduction of the Feynmann amplitude for the $q\rightarrow M'q'$ transition up to order $(v/c)^2$, obtaining

$$H=-\frac{i}{(2\pi)^{3/2}}\frac{1}{\sqrt{2\omega_\pi}}\frac{f_{\pi qq}}{m_\pi}F(k)\times\left[\vec{\sigma}\cdot\vec{k}-\frac{\omega_\pi}{2m_q}\vec{\sigma}\cdot(\vec{p}+\vec{p}\,')\right]\tau_\alpha^+\ \delta^{(3)}(\vec{p}\,'+\vec{k}-\vec{p}), \tag{12}$$

where $f_{\pi qq}=g_{ch}(m_\pi/2m_q)$, $\vec{p}$ $(\vec{p}\,')$ is the initial (final) quark momentum, $\vec{k}$ the pion momentum, $\omega_\pi=\sqrt{k^2+m_\pi^2}$ the pion energy, and $F(k)$ the πqq vertex form factor that fixes the chiral symmetry breaking scale.

To obtain the $B\rightarrow M'B'$ vertex function, one needs the baryon and meson wave functions. To be consistent with the resonating group method calculations, we assume that the spatial baryon wave function is given by Eq. (10) which, in momentum space and removing the center of mass motion, is expressed as

$$\phi_B(\vec{p}_{\xi_1},\vec{p}_{\xi_2})=\left[\frac{2b^2}{\pi}\right]^{3/4}e^{-b^2p_{\xi_1}^2}\left[\frac{3b^2}{2\pi}\right]^{3/4}e^{-(3b^2/4)p_{\xi_2}^2}. \tag{13}$$

The pion is considered as an elementary field. After integrating the spatial coordinates, one obtains an operator in the quark spin-isospin space which should be transformed into operators at the baryonic level to obtain the $\pi BB'$ vertex. Using the Appendix and summing in the recoupling coefficients, one arrives at the following expression for the πNN and the $\pi N\Delta$ vertex in the center of mass system:

$$\Gamma_{\pi NN}=-\frac{i}{(2\pi)^{3/2}}\frac{1}{\sqrt{2\omega_\pi}}\frac{f_{\pi NN}(k)}{m_\pi}\times(\tau_N)_\alpha^+\ \vec{\sigma}_N\cdot\vec{k}\ \ \delta^{(3)}(\vec{P}'+\vec{k}), \tag{14}$$

where $\vec{P}'$ is the momentum of the final nucleon, σ_N (τ_N) are the nucleon spin (isospin) operators, and the effective coupling constant is given by

$$f_{\pi NN}(k)=\frac{5}{3}f_{\pi qq}F(k)e^{-b^2k^2/6}\left(1+\frac{\omega_\pi}{6m_q}\right) \tag{15}$$

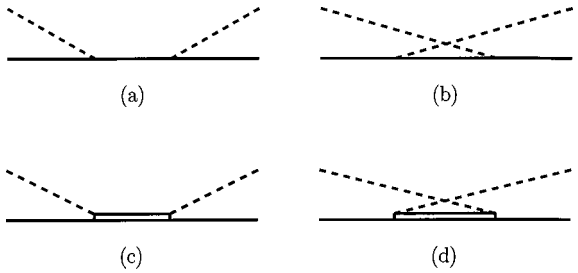

FIG. 1. Contributions to πN scattering. (a) and (b) correspond to processes with one N intermediate state whereas (c) and (d) have a Δ intermediate state.

and

$$\Gamma_{\pi N\Delta}=-\frac{i}{(2\pi)^{3/2}}\frac{1}{\sqrt{2\omega_\pi}}\frac{f_{\pi N\Delta}(k)}{m_\pi}\times(\tau_{N\Delta})_\alpha^+\vec{\sigma}_{N\Delta}\cdot\vec{k}\ \ \delta^{(3)}(P'+k), \tag{16}$$

where $\sigma_{N\Delta}(\tau_{N\Delta})$ are the $N-\Delta$ spin (isospin) transition operators defined in the Appendix and

$$f_{\pi N\Delta}(k)=2\sqrt{2}f_{\pi qq}F(k)e^{-b^2k^2/6}\left(1+\frac{\omega_\pi}{6m_q}\right). \tag{17}$$

For zero momentum transfer and neglecting relativistic corrections we recover the usual relation

$$f_{\pi N\Delta}^2=\frac{72}{25}f_{\pi NN}^2. \tag{18}$$

IV. THE P_{33} πN PHASE SHIFT

The P_{33} πN partial wave is dominated by the Δ resonance and, although it is not a very good test ground for pion-baryon interaction models, its calculation provides an excellent test of the expressions deduced in the previous section.

At tree level the πN potential should include all the diagrams containing one intermediate N or Δ (Fig. 1). However Fig. 1(a) only contributes to the P_{11} partial wave, whereas the crossed Δ, Fig. 1(d), has a negligible contribution. Therefore we will only include in our calculation Figs. 1(b) and 1(c).

Unitarity requires the scattering amplitude f_α to be a complex quantity. However, the scattering amplitude turns out to be real in a tree level approximation. Since we work in this approximation, we identify the scattering amplitude with the real K matrix, K_α, from which an f_α that recovers unitarity is obtained by

$$f_\alpha=\frac{K_\alpha}{1-i|k_0|K_\alpha}, \tag{19}$$

where k_0 denotes the πN relative momentum in its center of mass frame. At resonance the K_α matrix has a pole on the real axis at the Δ bare mass.

In the S matrix, this pole is shifted into the complex plane in such a way that the corresponding resonance width is in accordance with the unitarity condition. Then, this approximation is consistent with our assumption that the Δ mass is the bare mass. In case we have fully solved the scattering problem, the mass would change due to the renormalization process. Under these assumptions the K matrix can be written in a Born approximation as

$$K_{\pi N}^{P_{33}}(k,k') = \frac{1}{(2\pi)^3}\frac{1}{2\sqrt{\omega_\pi(k)\omega_\pi(k')}}\frac{f_{\pi N\Delta}(k)f_{\pi N\Delta}(k')}{m_\pi^2} \times\frac{4\pi}{3}\frac{k'k}{E_{\pi N}-m_\Delta} - \frac{1}{(2\pi)^3}\frac{1}{2\sqrt{\omega_\pi(k)\omega_\pi(k')}}\frac{f_{\pi NN}(k)f_{\pi NN}(k')}{m_\pi^2} \times 4\pi m_N\sum_l A_l Q_l(z) \quad (20)$$

with

$$A_l=(-1)^l 36(2l+1)\begin{pmatrix}1 & l & 1\\ 0 & 0 & 0\end{pmatrix}^2\begin{Bmatrix}1 & \frac{1}{2} & \frac{3}{2}\\ l & 1 & 1\\ 1 & \frac{1}{2} & \frac{1}{2}\end{Bmatrix}, \quad (21)$$

$$z=m_N\frac{m_N+\frac{k^2+k'^2}{2m_N}+\omega_\pi(k)+\omega_\pi(k')-E_{\pi N}}{kk'}, \quad (22)$$

and Q_l are the Legendre functions of the second kind. The first term on the right-hand side of Eq. (20) corresponds to Fig. 1(c) whereas the second one corresponds to Fig. 1(b). The phase shift is calculated in terms of the K matrix for an initial and final on-shell momentum given by

$$k_0^2=2m_N E_{\pi N}-2m_N\sqrt{2m_N E_{\pi N}-m_N^2+m_\pi^2}, \quad (23)$$

where $E_{\pi N}$ is the total πN center of mass energy.

The calculated P_{33} πN phase shift is compared to the experimental data in Fig. 2. The parameters used are taken from Ref. [3] and they are shown in Table I. They were fixed on the study of the NN system below pion threshold. The baryon spectrum has also been studied with these parameters by means of a Faddeev calculation [13,14]. The results, which are shown in Fig. 1 of Ref. [14], give a reasonable description of the experimental data. It is worthwhile to note that although no parameter is fitted to the πN data, the agreement with experiment is excellent. This gives us confidence to use the expression deduced for the $\pi N\Delta$ vertex to calculate the NN phase shifts above the pion threshold.

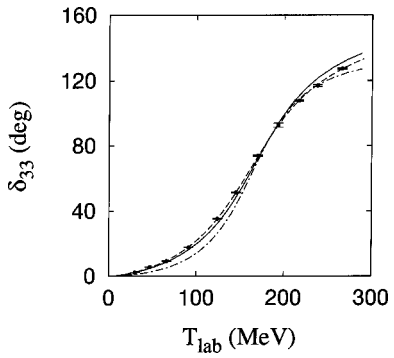

FIG. 2. The P_{33} πN phase shift. Experimental data are taken from the energy-independent (dots) and energy-dependent (dashed line) analysis of Arndt *et al.* (Ref. [20]). The dash-dotted line shows the result including only Fig. 1(c). The solid line corresponds to the result, also considering Fig. 1(b).

V. *NN* PHASE SHIFTS AND INELASTICITIES IN THE CCM

As explained in the Introduction we will solve the NN problem above pion threshold by means of the coupled-channel method. The starting point of the method is closely related to quark-model ideas, although it was developed at the baryon level. It makes the assumption that the nucleon is the ground state of a composite particle with excited states clearly identifiable. When two nucleons interact, one of them can be excited and decay into a πN state. The three-body problem is reduced to a two-body problem assuming that the $NN\to\pi NN$ transition only takes place through resonances. The effect of the coupling to resonances mainly depends on the strength and range of the transition potential. Therefore it is important to use a consistent interaction for the NN and $N\Delta$ channels, as is the case for the quark model used.

Other approaches appear in the literature and we will mention some of them for later comparison. Earlier works (Kloet and Tjon [15], VerWest [16]) performed coupled-channel calculations using NN and $N\Delta$ separable potentials. In this way they were able to solve analytically the Lippmann-Schwinger equation. The first calculation with realistic potentials was carried out by Lee [17], using the Paris potential with the $N\Delta$ box diagrams subtracted for the NN interaction, whereas the $NN\to N\Delta$ transition was represented by phenomenological π and ρ meson-exchange potentials. The model was later improved by including a $N\Delta$ retarded interaction. A similar model was developed by the Hannover

TABLE I. Quark-model parameters.

b (fm)	0.518
m_q (MeV)	313
Λ_χ (fm^{-1})	4.2997
m_{PS} (fm^{-1})	0.7
m_S (fm^{-1})	3.513
g_{ch}^2	6.6608
α_s	0.4977

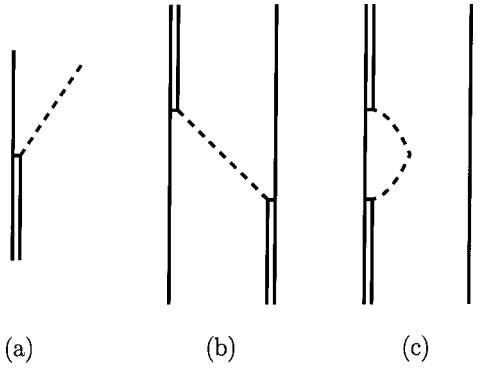

FIG. 3. (a) $\pi N\Delta$ vertex. (b) Retarded one-pion exchange diagram. (c) Δ self-energy diagram.

group also using the Paris potential for the NN interaction and an instantaneous potential which includes σ, π, ρ and ω mesons for the $N\Delta$ interaction [5,7,18]. Slightly different is the approach of Elster *et al.* in the framework of the Bonn potential model [19,20]. They used relativistic transition potentials evaluating the box diagrams $N\Delta$ and $\Delta\Delta$ with $\rho\pi$, $\pi\pi$, and $\rho\rho$ exchanges using time ordered perturbation theory. The self-energy diagrams of the nucleon and delta

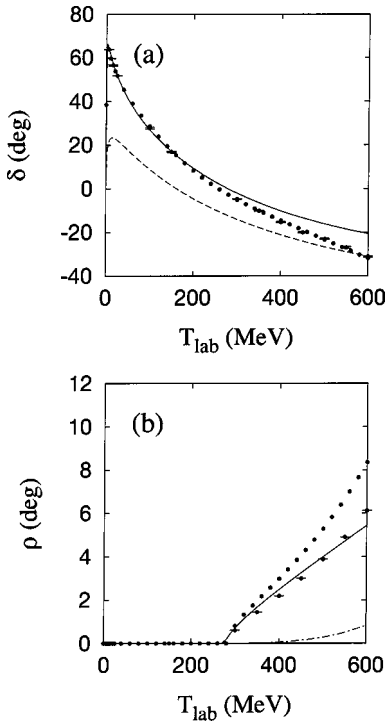

FIG. 4. (a) NN phase shift and (b) inelasticity for the $^1S_0$ partial wave. The experimental data correspond to the phase shift analysis of Arndt *et al.* (Ref. [20]). In (a), the dashed line shows the phase shift including only the NN channel. Solid and dash-dotted lines show the results including $N\Delta$ and $\Delta\Delta$ states for calculations 1 and 2, respectively. In (b), the dash-dotted line shows the inelasticity including the energy as well as the momentum dependence on the Δ width, whereas the solid line shows the result considering only the energy dependence.

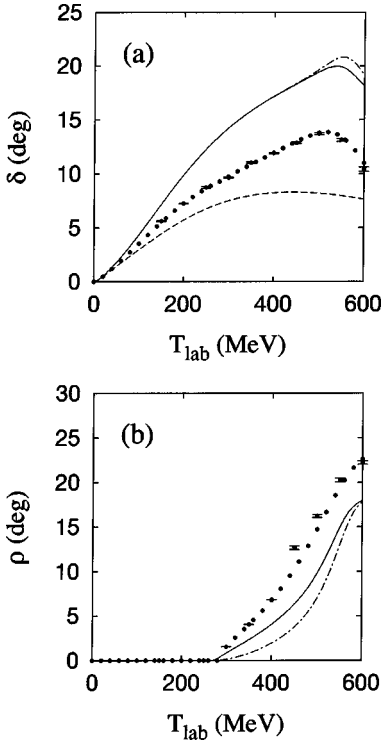

FIG. 5. Same as Fig. 4 for the $^1D_2$ NN partial wave.

were the sources of inelasticity.

As has been previously discussed, the inelasticity is predominantly single-pion production and occurs essentially in the isospin-triplet partial waves, therefore we will perform a NN-$N\Delta$ coupled-channel calculation. We start from the coupled set of Lippmann-Schwinger equations for the NN-$N\Delta$ system,

$$T_{NN}=V_{NN}+V_{NN}G_NT_{NN}+V_{N\Delta}G_\Delta T_{\Delta N}, \tag{24}$$

$$T_{\Delta N}=V_{\Delta N}+V_{\Delta N}G_NT_{NN}+V_{\Delta\Delta}G_\Delta T_{\Delta N}, \tag{25}$$

where V_{NN} represents the $NN\rightarrow NN$ potential, $V_{N\Delta}$ the $NN\rightarrow N\Delta$ transition, and $V_{\Delta\Delta}$ the $N\Delta\rightarrow N\Delta$ interaction. The main process for pion production is given by the $\pi N\Delta$ vertex depicted in Fig. 3(a), in which the Δ couples to a πN state. The introduction of this diagram has two consequences. The first one is that the $N\Delta\rightarrow N\Delta$ one-pion exchange potential has now a retarded interaction, shown in Fig. 3(b). As a consequence the $V_{\Delta\Delta}$ interaction would get modified. However, the diagonal $V_{\Delta\Delta}$ potential has a minor influence on the NN channels and we will not take this modification into account. The second one is the appearance of the delta self-energy diagram in the presence of a spectator nucleon shown in Fig. 3(c), which has a contribution to the Δ width and has to be added to the interaction. We denote by $v_\Delta^{se}(q)$ the Δ self-energy interaction,

$$v_\Delta^{se}(q)=\left\langle \gamma_\Delta\left|\frac{1}{E_\Delta(q)-\omega_\pi-\omega_N+i\varepsilon}\right|\gamma_\Delta\right\rangle, \tag{26}$$

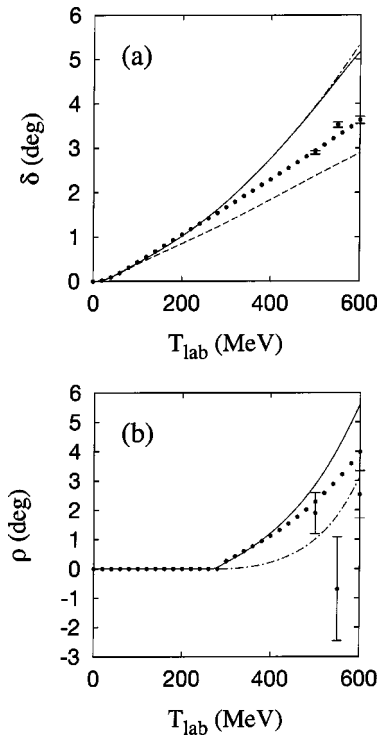

FIG. 6. Same as Fig. 4 for the ${}^1G_4$ NN partial wave.

where γ_Δ is the structure function of the $\pi N\Delta$ vertex. Thus, the coupled-channel problem now becomes

$$\tilde{T}=\tilde{V}+\tilde{V}^{se}+(\tilde{V}+\tilde{V}^{se})\tilde{G}\tilde{T}, \tag{27}$$

where $\tilde{T}$, $\tilde{V}$, $\tilde{V}^{se}$, and $\tilde{G}$ are two by two matrices corresponding to

$$\tilde{T}=\begin{pmatrix} T_{NN} & T_{N\Delta} \\ T_{\Delta N} & T_{\Delta\Delta} \end{pmatrix}, \quad \tilde{V}=\begin{pmatrix} V_{NN} & V_{N\Delta} \\ V_{\Delta N} & V_{\Delta\Delta} \end{pmatrix}, \tag{28}$$

$$\tilde{V}^{se}=\begin{pmatrix} 0 & 0 \\ 0 & v_\Delta^{se} \end{pmatrix}, \quad \tilde{G}=\begin{pmatrix} G_N & 0 \\ 0 & G_\Delta \end{pmatrix}. \tag{29}$$

Equation (27) can now be written as

$$\tilde{T}^D=\tilde{V}+\tilde{V}\tilde{G}^D\tilde{T}^D, \tag{30}$$

where

$$\tilde{T}=\tilde{G}^{-1}[\tilde{G}^D+\tilde{G}^D\tilde{T}^D\tilde{G}^D]\tilde{G}^{-1}-\tilde{G}^{-1} \tag{31}$$

with

$$\tilde{G}^D=\begin{pmatrix} G_N & 0 \\ 0 & G_\Delta^D, \end{pmatrix} \tag{32}$$

and $G_\Delta^D(E)$ is the dressed Δ propagator,

$$G_\Delta^D(E)=\frac{1}{E-(m_\Delta-m_N)-\dfrac{q^2}{2\mu_\Delta}-v_\Delta^{se}(q)+i\varepsilon}. \tag{33}$$

The NN phase shifts and inelasticities are obtained by solving the Lippmann-Schwinger equation with the renormalized Δ propagator. Since the vertex used in the Δ self-energy diagram is the one used in πN scattering, the value of the Δ width comes out consistent with experiment because we describe properly the P_{33} πN partial wave.

In Eq. (33) we use only the imaginary part of the Δ self-energy diagram which gives the Δ width. This is the reason, as in the case of the πN scattering, to use for m_Δ the physical mass. The Δ width is given by

$$\Gamma_\Delta=\frac{2}{3}\frac{f_{\pi N\Delta}^2(k_0)}{4\pi\ m_\pi^2}\frac{m_N}{\omega_\pi(k_0)+m_N}\ k_0^3 \tag{34}$$

with $\omega_\pi=\sqrt{m_\pi^2+k_0^2}$ the pion energy in the πN center of mass system and k_0 the relative momentum of the πN system given in terms of the center of mass energy $E_{\pi N}$ by Eq. (23). This is related with the NN center of mass energy by

$$S_{\pi N}=(\sqrt{S}-\sqrt{m_N^2+p^2})^2-p^2, \tag{35}$$

where $S_{\pi N}=E_{\pi N}^2$ is the invariant mass of the πN system, $\vec{p}$ is the relative momentum of the $N\Delta$ $[N(\pi N)]$ system, and S the invariant mass,

$$S=(2m_N+E_{\text{c.m.}})^2, \tag{36}$$

with $E_{\text{c.m.}}$ the kinetic center of mass energy of the NN system.

VI. RESULTS AND DISCUSSION

In this section we present the results obtained for the NN phase shifts and inelasticities with the model described above. The partial wave scattering amplitudes are related to the partial wave S_α matrix elements by

$$S_\alpha(E)=1+2iT_\alpha(E). \tag{37}$$

We will use for S_α the parametrization of Arndt and Roper [21],

$$S_\alpha=\cos^2\rho_\alpha e^{2i\delta_\alpha}, \tag{38}$$

and, therefore,

$$K_\alpha=\tan\delta_\alpha+i\tan^2\rho_\alpha \tag{39}$$

with δ_α and ρ_α the phase shift and the inelasticity, respectively, in the NN partial wave α.

The starting point of our calculation is the qq potential used previously to describe the NN phenomenology below the pion threshold. As already mentioned, we do not fit any parameter to data above the pion threshold. Since we only include the inelasticity due to the Δ self-energy only isospin-triplet partial waves are presented.

The results for the NN phase shifts and inelasticities are shown in Figs. 4–11 and compared to results from the energy-dependent and energy-independent partial wave analysis of Arndt *et al.* [22]. The experimental data, shown

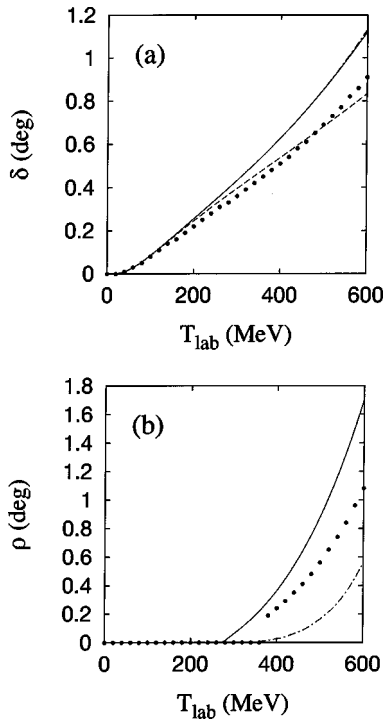

FIG. 7. Same as Fig. 4 for the ${}^1I_6$ NN partial wave.

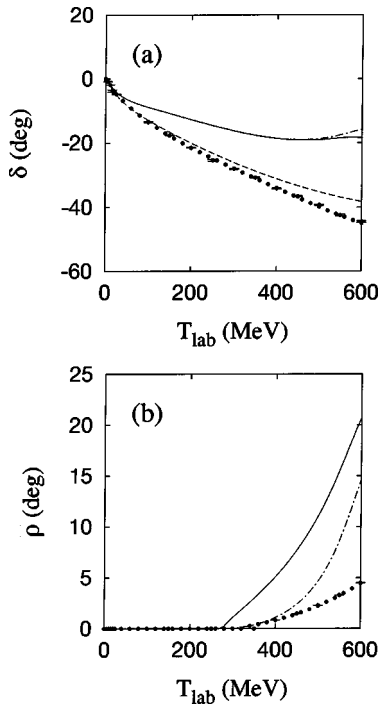

FIG. 9. Same as Fig. 4 for the ${}^3P_1$ NN partial wave.

by points, have been obtained from the interactive program SAID [23]. For the phase shifts, the solid line shows results for the coupled-channel calculation including $N\Delta$ and $\Delta\Delta$ intermediate states (although, as has been previously explained, the inelasticity is only included through the $N\Delta$ channel). Dashed lines refer to results including only the NN channel. For the inelasticities, the solid line shows the result including the energy dependent Δ width whereas dash-dotted lines include the energy and momentum dependence. The difference between these two approximations will be discussed later.

As a general trend the experimental phase shifts are reasonably well reproduced by our calculation except for the P

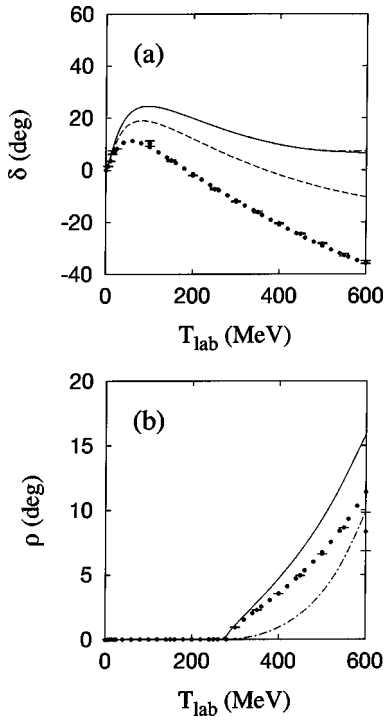

FIG. 8. Same as Fig. 4 for the ${}^3P_0$ NN partial wave.

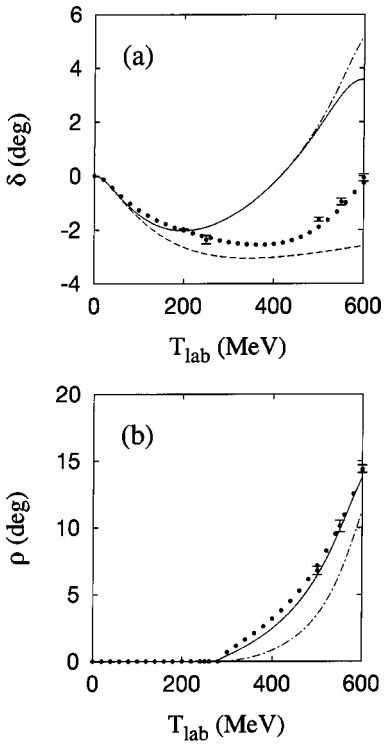

FIG. 10. Same as Fig. 4 for the ${}^3F_3$ NN partial wave.

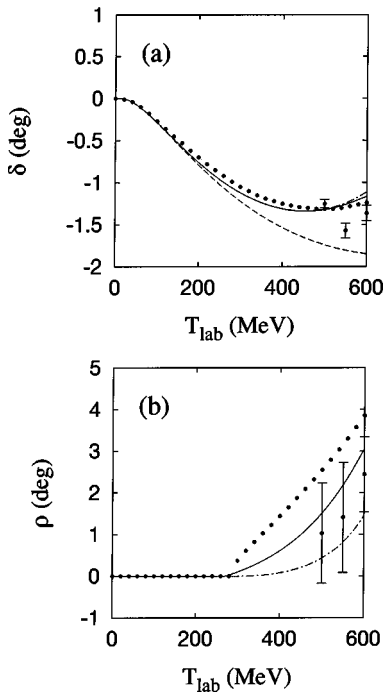

FIG. 11. Same as Fig. 4 for the $^3H_5$ NN partial wave.

waves, which due to the lack of spin-orbit interaction are overestimated, as is the case below the pion threshold. The influence of the $N\Delta$ channel is more important for the low angular momentum partial waves.

The most interesting isospin-triplet partial waves are the $^1D_2$ and $^3F_3$, because the $NN-N\Delta$ coupling is very important. The Argand plot for both cases, Fig. 12, presents a counterclockwise behavior with increasing energy, which is considered to be a signal of a possible resonance. As seen in Figs. 5 and 10, the resonant behavior observed in the experimental data only appears when the coupling to the $N\Delta$ channel is considered. In both cases our calculation overestimates the phase shifts which is already known for models including only $N\Delta$ channels.

The resonant behavior of these two partial waves has been extensively discussed in the literature. The first interpretation in terms of dibaryon resonances was given by Hoshizaki [24] who parametrized the S matrix including a Breit-Wigner resonance part. He obtained 2.17 GeV and 2.22 GeV for the masses of the $^1D_2$ and $^3F_3$ dibaryons, respectively. Later on it was shown that the resonant behavior could also be explained as an effect of the opening of the $N\Delta$ threshold. In our case the $^1D_2$ NN partial wave is coupled to the $^5S_2$ $N\Delta$ partial wave, which in our model has a very weak bound state [25]. The energy of the bound state is 0.141 MeV below the $N\Delta$ threshold which gives a mass of 2.17 GeV for this state, in agreement with the value obtained by Hoshizaki. Since the effect of the threshold is always present, one should conclude that in our model the resonant behavior of the $^1D_2$ partial wave is a combined effect.

As mentioned before, we performed two different calculations. In the first one, we only introduced the energy dependence when we calculated the Δ width, which we will call calculation 1, whereas in the other we considered the

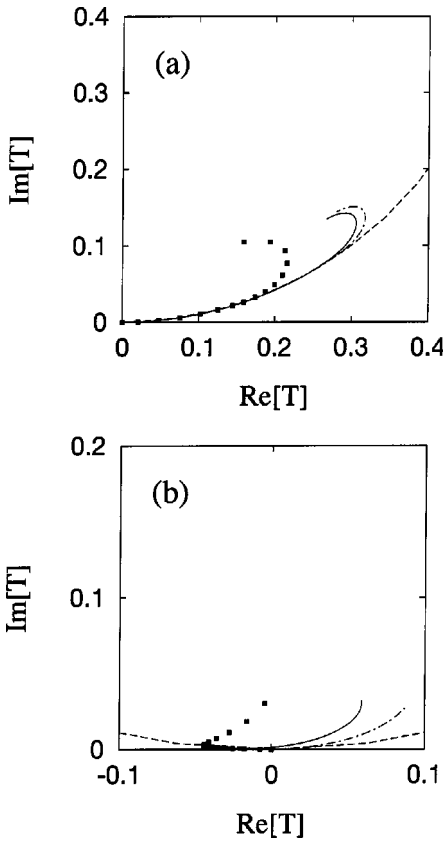

FIG. 12. Argand diagram of the T-matrix amplitudes for the (a) $^1D_2$ and (b) $^3F_3$ NN partial waves. We show by squares the experimental data of Arndt *et al.* (Ref. [20]). The solid line shows the result for calculation 1 and the dash-dotted line for calculation 2. The dashed line represents the unit circle.

energy and momentum dependence, being referred to as calculation 2. This different treatment of the Δ width has a very small effect on the phase shifts but it is very important for the inelasticities as seen in the figures. This can be understood in the following way. When the momentum dependence is not included the value of the Δ width for zero relative momentum is taken for all relative momenta. This is its maximum value, as shown in Fig. 13, where Γ_Δ is plotted as a function of the energy of the NN system and the momen-

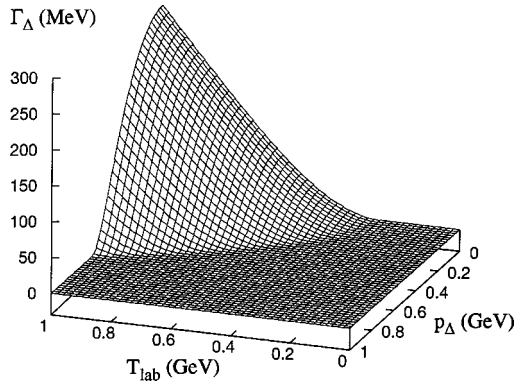

FIG. 13. Δ width as a function of the NN energy in the laboratory system and the momentum of the Δ.

tum of the Δ. Therefore, for a fixed NN energy if we increase the momentum, the energy available for the decay (energy in the πN center of mass system) decreases and consequently so does the Δ width. This is why the inelasticity is always smaller for calculation 2. Similar results were already obtained by Kloet and Tjon [15] and Elster *et al.* [20]. The inelasticity in the $^1S_0$ channel decreases too much when the momentum dependence on the Δ width is included whereas for the other partial waves the experimental data lie between the two calculations.

VII. SUMMARY

We have performed a calculation of the NN phase shifts and inelasticities above the pion threshold within a chiral quark model in the framework of the CCM. The only source of inelasticity considered has been the Δ self-energy diagram that provides the Δ width. This is the main inelastic contribution found in other models at baryon level and no important differences should be expected if other contributions are included.

The phase shifts are reasonably well reproduced, although the coupling to $N\Delta$ and $\Delta\Delta$ states gives in general too much attraction. The effect of the $N\Delta$ channel is more important than the one from the $\Delta\Delta$ channel. This was already observed in our calculation below the pion threshold. The inelasticities obtained are small when the momentum dependence of the Δ width is included.

Although the quantitative description of the phase shifts is not as good as in other models at baryon level, we want to emphasize that our calculation above pion threshold is parameter-free in the sense that all the parameters of the model are fixed from the study of data below pion threshold. The $\pi N\Delta$ vertex as well as the potentials including resonances are calculated from the same model as the NN potential. To our knowledge this is the first calculation of the NN system above the pion threshold making use only of interactions derived from a quark model.

We have studied the isospin-triplet partial waves. For isospin-singlet partial waves, $\Delta\Delta$ states would be a source of inelasticity, however, for these channels the coupling to the Roper resonance is more important because its pion production threshold is at lower energy. Work with the inclusion of $NN^*(1440)$ intermediate states is now in progress.

ACKNOWLEDGMENTS

This work has been partially funded by the Ministerio de Ciencia y Tecnología under Contract No. BFM2001-3563, by Junta de Castilla y León under Contract No. SA-109/01, and by the Ramón Areces Foundation (Spain).

APPENDIX: EFFECTIVE COUPLING CONSTANTS

In this appendix we deduce the effective πNN and $\pi N\Delta$ coupling constants from the πqq vertex. We start from the Hamiltonian of Eq. (12) and we take the expectation value between baryon wave functions. Since the contributions of the three quarks are equal, we calculate for quark three and multiply by 3. For the spatial part we use the wave function given in Eq. (13). In this way we get the following operator in the spin-isospin-color space of quark three:

$$\tilde{H}=-\frac{3i}{(2\pi)^{3/2}}\frac{1}{\sqrt{2\omega_\pi}}\frac{f_{\pi qq}}{m_\pi}\ \vec{\sigma}_3\cdot\left[\vec{k}\left(1+\frac{\omega_\pi}{6m_q}\right)-\frac{\omega_\pi}{3m_q}\vec{P}\right]\times(\tau_{\alpha_3})^+e^{-b^2k^2/6}\ \ \delta^{(3)}(\vec{P}'-\vec{P}+\vec{k}). \tag{A1}$$

The vertices at baryon level are obtained relating the expectation value of the quark operators with those at baryon level. We finally get for the πNN vertex

$$\Gamma_{\pi NN}=-\frac{3i}{(2\pi)^{3/2}}\frac{1}{\sqrt{2\omega_\pi}}\frac{f_{\pi qq}}{m_\pi}\times e^{-b^2k^2/6}(\tau_{\alpha_N})^+\vec{\sigma}_N\cdot\left[\vec{k}\left(1+\frac{\omega_\pi}{6m_q}\right)-\frac{\omega_\pi}{3m_q}\vec{P}\right]\times\delta^{(3)}(\vec{P}'-\vec{P}+\vec{k})\ \ 2\sum_{l=0,1}\begin{Bmatrix}1 & \frac{1}{2} & \frac{1}{2}\\ l & \frac{1}{2} & \frac{1}{2}\end{Bmatrix}^2 \tag{A2}$$

and for the $\pi N\Delta$ one,

$$\Gamma_{\pi N\Delta}=-\frac{3i}{(2\pi)^{3/2}}\frac{1}{\sqrt{2\omega_\pi}}\frac{f_{\pi qq}}{m_\pi}\times e^{-b^2k^2/6}(\tau_{N\Delta})^+_\alpha\vec{\sigma}_{N\Delta}\cdot\left[\vec{k}\left(1+\frac{\omega_\pi}{6m_q}\right)-\frac{\omega_\pi}{3m_q}\vec{P}\right]\ \ \delta^{(3)}(\vec{P}'-\vec{P}+\vec{k})\times 2\left\langle\frac{1}{2}\middle\|\sigma_3\middle\|\frac{1}{2}\right\rangle\left\langle\frac{1}{2}\middle\|\tau_3\middle\|\frac{1}{2}\right\rangle\begin{Bmatrix}1 & \frac{1}{2} & \frac{3}{2}\\ l & \frac{1}{2} & \frac{1}{2}\end{Bmatrix}^2, \tag{A3}$$

where we use the NN to $N\Delta$ spin transition operator defined by

$$\langle m_{s_\Delta}|\sigma^\mu_{N\Delta}|m_{s_N}\rangle=\sqrt{2s_\Delta+1}\times(-1)^{1-s_N-m_{s_\Delta}}\begin{pmatrix}s_N & 1 & s_\Delta\\ m_{s_N} & \mu & -m_{s_\Delta}\end{pmatrix} \tag{A4}$$

and analogously for the isospin operator. Therefore the effective coupling constants are given by

$$f_{\pi NN}(k)=6f_{\pi qq}e^{-b^2k^2/6}\left(1+\frac{\omega_\pi}{6m_q}\right)\sum_{l=0,1}\begin{Bmatrix}1&\frac{1}{2}&\frac{1}{2}\\ l&\frac{1}{2}&\frac{1}{2}\end{Bmatrix}^2,$$

$$f_{\pi N\Delta}(k)=3\sqrt{2}f_{\pi qq}e^{-b^2k^2/6}\left(1+\frac{\omega_\pi}{6m_q}\right)\left\langle\frac{1}{2}\middle\|\sigma_3\middle\|\frac{1}{2}\right\rangle \times\left\langle\frac{1}{2}\middle\|\tau_3\middle\|\frac{1}{2}\right\rangle\begin{Bmatrix}1&\frac{1}{2}&\frac{3}{2}\\ l&\frac{1}{2}&\frac{1}{2}\end{Bmatrix}^2. \quad \text{(A5)}$$

[1] M. Oka and K. Yazaki, Prog. Theor. Phys. **66**, 556, 572 (1980); A. Faessler, F. Fernández, G. Lübeck, and K. Shimizu, Phys. Lett. **122B**, 201 (1982).

[2] F. Fernández, A. Valcarce, U. Straub, and A. Faessler, J. Phys. G **19**, 2013 (1993).

[3] D.R. Entem, F. Fernández, and A. Valcarce, Phys. Rev. C **62**, 034002 (2000).

[4] M. Furuichi and K. Shimizu, Phys. Rev. C **65**, 025201 (2002); H. Garcilazo, A. Valcarce, and F. Fernández, *ibid.* **64**, 058201 (2001).

[5] A. Valcarce, F. Fernández, H. Garcilazo, M.T. Peña, and P.U. Sauer, Phys. Rev. C **49**, 1799 (1994).

[6] H. Garcilazo and T. Mizutani, *πNN Systems* (World Scientific, Singapore, 1990).

[7] H. Pöpping, P.U. Sauer, and Z. Xi-Zhen, Nucl. Phys. **A474**, 557 (1987).

[8] D. Diakonov, in *Selected Topics in Nonperturbative QCD*, edited by A. DiGiacomo and D. Diakonov (IOS Press, Amsterdan, 1996), pp. 397–432.

[9] J.I. Skullerud and A.G. Williams, Nucl. Phys. **B83-84**, 209 (2000).

[10] A. Manohar and H. Georgi, Nucl. Phys. **B234**, 189 (1984).

[11] A. de Rújula, H. Georgi, and S.L. Glashow, Phys. Rev. D **12**, 147 (1975).

[12] A. Le Yaouanc, L.L. Oliver, O. Pène, and J.-C. Raynal, *Hadron Transitions in the Quark Model* (Gordon and Breach, New York, 1988).

[13] H. Garcilazo, A. Valcarce, and F. Fernández, Phys. Rev. C **63**, 035207 (2001).

[14] H. Garcilazo, A. Valcarce, and F. Fernández, Phys. Rev. C **64**, 058201 (2001).

[15] W.M. Kloet and J.A. Tjon, Phys. Lett. **99B**, 80 (1981); **106**, 24 (1981).

[16] B.J. VerWest, Phys. Rev. C **25**, 482 (1982).

[17] T.-S.H. Lee, Phys. Rev. Lett. **50**, 1571 (1983).

[18] M.T. Peña, H. Garcilazo, U. Oelfke, and P.U. Sauer, Phys. Rev. C **45**, 1487 (1992).

[19] Ch. Elster, W. Ferchländer, K. Holinde, D. Schütte, and R. Machleidt, Phys. Rev. C **37**, 1647 (1988).

[20] Ch. Elster, K. Holinde, D. Schütte, and R. Machleidt, Phys. Rev. C **38**, 1828 (1988).

[21] R.A. Arndt and L.D. Roper, Phys. Rev. D **25**, 2011 (1982).

[22] R.A. Arndt, C.H. Oh, I.I. Strakovski, R.L. Workman, and F. Dohrmann, Phys. Rev. C **56**, 3005 (1997).

[23] PWAs can be accessed via a ssh/telnet call to the SAID facility gwdac.phys.gwo.edu with userid: said (no password), or a link to the website http://gwdac.phys.gwu.edu

[24] N. Hoshizaki, Prog. Theor. Phys. **60**, 1796 (1978); **61**, 129 (1979).

[25] R.D. Mota, A. Valcarce, F. Fernández, D.R. Entem, and H. Garcilazo, Phys. Rev. C **65**, 034006 (2002).